AD-A080 908 NATIONAL BUREAU OF STANDARDS WASHINGTON DC SURFACE S--ETC F/G 20/2
THE ROLE OF STEPS AND DEFECTS IN ELECTRON STIMULATED DESORPTION--ETC(U)
JAN 80 T E MADEY N00014-80-F-0002
UNCLASSIFIED TR-10 NL

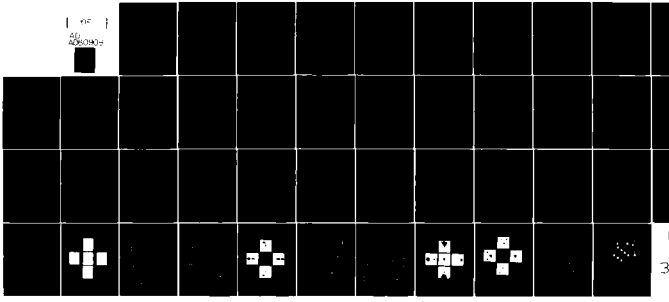

END
DATE FILMED
3-80
DDC

OFFICE OF NAVAL RESEARCH

Contract N00014-80-F-0002

TECHNICAL REPORT NO. 10

THE ROLE OF STEPS AND DEFECTS IN ELECTRON STIMULATED DESORPTION: OXYGEN ON STEPPED W (110) SURFACES

By

Theodore E. Madey
Surface Science Division
National Bureau of Standards
Washington, D. C. 20234

20 January 1980

To be published in Surface Science

SECURITY CLASSIFICATION OF THIS PAGE (When Data Entered)

REPORT DOCUMENTATION PAGE

READ INSTRUCTIONS BEFORE COMPLETING FORM

1. REPORT NUMBER: Technical Report No. 10
2. GOVT ACCESSION NO.:
3. RECIPIENT'S CATALOG NUMBER:

4. TITLE (and Subtitle): The Role of Steps and Defects in Electron Stimulated Desorption: Oxygen on Stepped W (110) Surfaces
5. TYPE OF REPORT & PERIOD COVERED: Interim Technical
6. PERFORMING ORG. REPORT NUMBER: Rept 13

7. AUTHOR(s): Theodore E. Madey
8. CONTRACT OR GRANT NUMBER(s): N00014-80-F-0002

9. PERFORMING ORGANIZATION NAME AND ADDRESS: Surface Science Division, National Bureau of Standards, Washington, DC 20234
10. PROGRAM ELEMENT, PROJECT, TASK AREA & WORK UNIT NUMBERS: 11 20 Jan 81

11. CONTROLLING OFFICE NAME AND ADDRESS: Office of Naval Research, Physical Program Office, Arlington, VA 22217
12. REPORT DATE: January 20, 1980
13. NUMBER OF PAGES:

14. MONITORING AGENCY NAME & ADDRESS (if different from Controlling Office): 14) TR-10 12) 57
15. SECURITY CLASS. (of this report): Unclassified
15a. DECLASSIFICATION/DOWNGRADING SCHEDULE:

16. DISTRIBUTION STATEMENT (of this Report)

approved for Public Release; Distribution Unlimited

17. DISTRIBUTION STATEMENT (of the abstract entered in Block 20, if different from Report)

18. SUPPLEMENTARY NOTES

To be published in Surface Science.

19. KEY WORDS (Continue on reverse side if necessary and identify by block number)

Surface, adsorption, desorption, electron stimulated desorption, surface structure, stepped surfaces, defects, oxygen, tungsten.

20. ABSTRACT (Continue on reverse side if necessary and identify by block number)

In order to examine the role of atomic steps and defects on electron stimulated desorption (ESD) phenomena, we have studied the adsorption of oxygen on a polyhedral tungsten crystal containing a W(110) flat and 4 flats having orientations 6° and 10° off the (110) plane with rows of steps parallel to the [100] and [110] directions. Upon adsorption at 300K, there is little or no ESD O+ emission from the oxygen-covered (110) plane. In contrast, the stepped surfaces yield intense O+ emission normal to the terraces and in

DD FORM 1 JAN 73 1473 EDITION OF 1 NOV 65 IS OBSOLETE
S/N 0102-014-6601

SECURITY CLASSIFICATION OF THIS PAGE (When Data Entered)

420655

"downstep" directions, as seen using electron stimulated desorption ion angular distributions (ESDIAD). The presence of atomic steps has a major influence on sticking probability, saturation oxygen coverage and the ESDIAD patterns at all adsorption temperatures in the range 100K to ≳1400K. Adsorption at low coordination sites appears to be a key factor in producing high ESD ion yields.

THE ROLE OF STEPS AND DEFECTS IN ELECTRON STIMULATED DESORPTION: OXYGEN ON STEPPED W (110) SURFACES

Theodore E. Madey
Surface Science Division
National Bureau of Standards
Washington, D. C. 20234

ABSTRACT

In order to examine the role of atomic steps and defects on electron stimulated desorption (ESD) phenomena, we have studied the adsorption of oxygen on a polyhedral tungsten crystal containing a W(110) flat and 4 flats having orientations 6° and 10° off the (110) plane with rows of steps parallel to the [100] and [110] directions. Upon adsorption at 300K, there is little or no ESD O^+ emission from the oxygen-covered (110) plane. In contrast, the stepped surfaces yield intense O^+ emission normal to the terraces and in "downstep" directions, as seen using electron stimulated desorption ion angular distributions (ESDIAD). The presence of atomic steps has a major influence on sticking probability, saturation oxygen coverage and the ESDIAD patterns at all adsorption temperatures in the range 100K to ≥1400K. Adsorption at low coordination sites appears to be a key factor in producing high ESD ion yields.

I. Introduction

Single crystal surfaces containing a regular array of atomic steps have been shown in a variety of experiments to exhibit unique physical, chemical and electronic properties.[1-3] Surfaces vicinal to (i.e., with an orientation close to) the close packed W(110) surface have been of particular interest to a variety of investigators. LEED studies have demonstrated that the steps on W(110) vicinals are invariably monatomic in height[4, 5], and work function methods have been employed to determine the dipole moments of atoms at step edges.[6] The kinetics of adsorption and desorption of oxygen[5, 7] and nitrogen[8] as well as the LEED domain structures due to adsorbed overlayers[5] are sensitive to step density and geometry.

In a series of papers involving the use of the electron stimulated desorption (ESD) method to characterize the adsorption of oxygen on polycrystalline and single crystal tungsten surfaces (9-13 and references therein), it has generally been found that (a) little or no O^+ ion signal is liberated from the surface for oxygen coverages $\lesssim$ 0.5 monolayers, and (b) the O^+ ion signal rises precipitously as the oxygen coverages increases beyond this value. In a related study, the electron stimulated desorption ion angular distribution (ESDIAD) method was used to examine oxygen adsorption on a stepped W(110) crystal.[14] At low oxygen coverages, no O^+ ESD signal was seen. The intense O^+ ion beams observed at high coverages appeared to be directly related to the presence of surface steps.

The present work was undertaken in order to systematically examine the role of surface steps (and defects) of differing geometry on ESD phenomena. To this end, we have studied the adsorption of oxygen on a polyhedrally shaped tungsten crystal. It contains a flat (110) face and four different stepped vicinal surfaces having two different edge structures, each with two different step densities.[15] As pointed out by Besocke and Berger,[7] there are distinct advantages to using one polyhedrally shaped sample instead of many separately prepared crystals: (a) all surfaces are prepared on a single sample crystal with the same bulk impurity levels, (b) cleaning, heating and dosing of the sample is the same for all surfaces, so that good relative measurements can be made.

The general conclusions of this work are that (1) there is little O^+ ESD signal from a flat (110) surface, even at high coverages, (2) the surface sites from which the ESD O^+ signals originate are predominantly located at steps and defects, (3) ESDIAD is very sensitive to the local step geometry, (4) the temperature of adsorption has a major influence on the details of the adsorbed structures and resultant ESDIAD patterns.

II. Experimental

The sample was prepared from a high purity W single crystal using spark erosion and polishing techniques[15, 16], and is schematically shown in Fig. 1. The orientation of the central facet was checked at NBS using Laue x-ray back reflection, and found to be within 0.3° of the (110) plane. The angular orientations of the other facets with respect to the central (110) surface were determined using a back-reflected laser beam. The surrounding four facets are cut at (nominal) angles of 6° and 10° with respect to the central (110) plane. This resulted in stepped surfaces with two different edge orientations running parallel to the [110] and [100] directions, and two different step densities. The parameters which characterize the sample are shown in Table I, and are similar to (but not identical to) those of Ref. (7). Note that we use the nomenclature introduced by Lang et al.[17] to describe the stepped surfaces (W(S)-[8(110) x (112)] means a stepped tungsten surface; the average step contains 8 rows of atoms on a terrace of (110) orientation; the edge orientation is (112)). The letter labels T (top), C (center), B (bottom), L (left), and R (right) are a guide to the orientation of the LEED and ESDIAD patterns in the remainder of this paper.

The sample had a diameter of 7 mm and a thickness of about 2 mm. The smallest facet (the central (110) plane) measured 2 mm x 2 mm. The sample was mounted on a manipulator in a W wire support frame, was heated to 2500K

by electron bombardment from a planar filament behind the sample ($\gtrsim$250 watts), and could be cooled cryogenically to $\sim$ 100K. Temperatures were measured using a W/3% Re vs. W/26% Re thermocouple wire clamped between the sample and the support wire.

The sample and manipulator were used in an ultrahigh vacuum system which has been described previously.[14] The base pressure after bakeout was 1×10^{-10} torr. It is an ion pumped and Ti sublimation-pumped system containing a low energy electron gun, ESDIAD/LEED optics, cylindrical mirror analyzer for Auger electron spectroscopy (AES), quadrupole mass spectrometer (QMS), and gas inlet valves. In operation, a focused electron beam (<1 mm diameter, 100 to 400 eV) bombards the sample surface onto which gas has been adsorbed. The ion beams which desorb from the surface by electron stimulated desorption (ESD) pass through 2 hemispherical grids and are accelerated to a microchannel plate (MCP) assembly. The output electron signal from the MCP assembly (gain $\sim 10^6$) is displayed visually on a fluorescent screen. By reversing potentials on the MCP assembly, the LEED pattern from the surface is displayed. All of the LEED and ESDIAD patterns in this paper were photographed from the fluorescent screen. To study the different facets, it was necessary to employ both electron beam deflection and sample translation using the manipulator. Mass identification of ESD ions is done by rotating the sample to face the QMS. Angular profiles of ESD beams are made by monitoring the QMS ion yield as a function of ion desorption angle as the sample is rotated.

For most of the ESDIAD patterns presented in this paper, a bias potential of V_B = +200 V was applied to the sample to "compress" the ion trajectories so that all beams are visible on the screen. The total electron energy V_e in these cases is the electron gun potential plus the bias potential, V_e = 300 eV.

The crystal was cycled repeatedly in 10^{-6} torr of oxygen between 300K and 2500K in order to remove impurity C; oxygen was removed at 2200K. Comparison of typical carbon Auger signals from the clean (110) crystal with the carbon Auger signal from a saturation CO layer indicated that, at most, less than a few percent of a carbon monolayer was present prior to O_2 exposure for any of the measurements reported here. Carbon was more persistent on the stepped surfaces than on the flat (110). AES measurements on different facets were made by translating the crystal in front of the analyzer (rather than deflecting the beam) so as to minimize electron optical problems in Auger electron energy analysis.

Prior to an oxygen exposure (at pressures ranging from 4×10^{-9} torr to 5×10^{-7} torr), the titanium sublimation pump was flashed. This insured that the O_2/CO ratio as determined using the QMS was 100 or higher. Pressures were read using an uncalibrated nude ionization gauge.

III. Results

A. Clean Surface

Fig. 2 is a drawing of an idealized, unreconstructed W(110) crystal surface showing the atomic structure of the steps which are parallel to the

[100] and [110] directions, respectively. This model is oriented in the same way as the subsequent LEED and ESDIAD patterns. Note the more open structure of the steps at the top (and bottom), parallel to the [110] directions; the edge atoms are spaced 4.466 Å apart. By comparison, the edge atoms parallel to [100] directions have the spacing of the W lattice constant, 3.158 Å. The atom density of a perfect W(110) plane is 14.2×10^{14} atoms/cm^2.

The LEED patterns characteristic of the clean facets are shown in Fig. 3 for an electron energy of 110 eV. The patterns were all sharp, with low background intensity. The LEED pattern from the (110) flat is shown in the center, and the LEED patterns from the stepped surfaces surrounding the central (110) display the characteristic beam splitting.[1-3] These patterns are in excellent agreement with the work of Besocke and Berger.[7] It has been previously determined using LEED[4, 5] that the steps on thermally annealed tungsten (110) vicinal planes are monatomic in height.

B. Adsorption of Oxygen at 300K: Auger Measurements

In previous studies of the adsorption of oxygen on stepped W(110) vicinal surfaces, Engel et. al.[5] reported that the sticking coefficient on surfaces having steps parallel to the densely packed [111] direction did not differ markedly from the flat (110) surface. In contrast, Besocke and Berger[7] reported that (110) vicinal surfaces with steps parallel to [110] and [100] directions had higher sticking probabilities than the W(110) flat.

In order to verify the data of Ref. (7) with respect to adsorption kinetics, and to provide a coverage scale for the ESDIAD measurements, we have measured oxygen uptake on the five facets of the W polyhedron as a function of exposure using AES.

For the determination of oxygen adsorption kinetics, the clean polyhedral W crystal was exposed to successive doses of O_2. Following each exposure, the peak-to-peak height of the derivative oxygen (KVV) AES signal was recorded for each facet. The "on" time for the 2 kv defocussed AES beam for each measurement was $\lesssim$30s, during which time ESD effects were ascertained to be negligible. The maximum variation in W AES signal intensities was $\pm$5% between different facets; the oxygen Auger sensitivities were presumed to be independent of oxygen coverage on each facet, and were presumed to vary in proportion to the W, and the oxygen intensities were corrected accordingly. The normalized O (KVV) Auger signal is plotted vs. oxygen exposure for each of the facets in Fig. 4. The adsorption temperature was $\gtrsim$300 K. All of the plotted data were obtained for a single exposure run, but the curves were found to be reproducible. Although the O(KVV) signal is plotted in normalized fashion, the ordinate scale is quite close to the oxygen coverage, expressed in monolayers; the reasons for this are discussed below.

The data of Fig. 4 are in remarkably good agreement with those of Besocke and Berger[7]: the initial slopes and the final coverages are in the same order, and the curve for the B facet, W(S) - [8(110) x (112)], crosses over that of the R facet, W(S) - [10(110) x ($1\bar{1}0$)]. The only substantial

difference is that the data for the T facet is virtually identical to that of B. Besocke and Berger found that the data for their facet which most closely resembled our T facet, W(S) - [15(110) x (112)], had a lower initial slope and final coverage. The present data are reproducible to within ±5% at different points on the facet, and no apparent reason can be cited for this systematic difference. The highest coverage seen in Fig. 4 is for the L facet. Because the maximum coverage on L is already attained at ∿5L and does not vary with increasing exposure, and because the (110) plane has a very low sticking probability for coverages in excess of 0.5 monolayers[5, 7, 11], i.e., 7.1×10^{14} oxygen atoms/cm^2, the maximum coverage on Facet L is consistent with a coverage of one monolayer.

The LEED behavior on all facets was similar to the observations of Ref. 7. On the central W(110) C facet, the p(2 x 1) structure was sharp and intense at 20L exposure. On all the other facets, the p(2x1) structure reached its maximum intensity at lower exposures and had virtually disappeared at 20L.

The relative initial sticking probabilities, s/s_{max}, are proportional to the initial slopes of the Fig. 4 curves, and are given in Table II. $(s)_{max}$ is the initial sticking probability on the L facet, W(S) - [6(110) x ($1\bar{1}0$)]. These data substantiate the observations of Ref. (7) that compared to the flat (110) surface, the steps cause an increase in sticking probability. In addition to acting as local adsorption sites, the steps also facilitate the adsorption of oxygen on the terraces. Because of the presence of the steps, the oxygen coverage on the (110) terraces of each of the vicinal surfaces is higher than on the (110) flat (for oxygen exposures <20L).

C. Adsorption of Oxygen at 100K: Auger Measurements

The O(KVV) oxygen signal vs. oxygen exposure for adsorption at ~100K is shown in Fig. 5. The ordinate is normalized to the oxygen Auger signal observed for the L facet at 300K, 20L. As in the case of the 300K adsorption, the highest limiting coverage is found for the L facet and the lowest for the C, W(110) facet. There are smaller differences in initial slope (initial sticking probability) than at 300K, and the range of limiting coverages is smaller. It is particularly interesting to note that the limiting coverage on the C facet, W(110), is higher than at 300K whereas the limiting coverage on the L facet, W(S)-[6(110) x ($1\bar{1}0$)], is lower than at 300K. The differences between the oxygen adsorption behavior at 300K and 100K are related in part to the lack of mobility of oxygen at 100K. A direct manifestation of the relative lack of mobility at 100K is the observation that the p(2 x 1) LEED pattern is not seen on any of the facets during low temperature adsorption. Only after heating to T >200K do ordered overlayer LEED patterns emerge.

LEED also provides evidence for a higher limiting oxygen coverage at low temperature on the central W(110) facet C. Following adsorption (20L exposure) at 300K, the familiar p(2 x 1) pattern is seen; the optimal coverage for the p(2 x 1) structure is 0.5 monolayer[11, 12, 18, 19]. After a 20L exposure at 100K followed by heating to $T \gtrsim 300K$, the p(2 x 2) structure appears, which is known to correspond to $\theta \lesssim 0.75$ monolayers of oxygen[18,19].

D. Adsorption of oxygen at 300K: ESDIAD

For oxygen exposures <1L on the clean sample at 300K (i.e., for oxygen coverages less than a few tenths of a monolayer), there was little or no ion emission seen in ESDIAD study of any of the facets. Above this exposure, dim, off-normal beams oriented in the down-step direction along [110] azimuth were seen from the R and L facets, and a hint of down-step emission was also seen on the T and B facets. As the exposure increased these beams all became sharp and well-focussed, and beams normal to the terraces of the vicinal facets also appeared. Fig. 6 contains an array of ESDIAD patterns observed following an oxygen exposure of 4 L. The T and B patterns, each containing a beam normal to the (110) terraces and two down-step beams, are virtually identical to the patterns observed from the less highly stepped W(110) crystal which had been studied previously[14], and which also had steps parallel to the [110] direction. The R and L patterns are characterized by an elongated central spot, as well as several down-step beams, the brightest of which is along the [110] azimuth. On the R facet, the emission normal to the (110) terraces is to the right of the horizontally elongated central beam, i.e., approximately in the geometric center of the photograph; similarly, normal emission from the L facet is to the left of the elongated central beam. In both of these cases, there is an up-step contribution to the ion emission evident in the elongation of the central beam. The dominant impression upon looking at these patterns is that they are all characterized by normal and down-step

emission, with the only up-step emission seen on R and L facets.

At higher exposure (up to 40L) the patterns simply increased in intensity. No new beams were seen on T or B; the beams oriented off the [110] azimuth increased in intensity on R and L facets and additional up-step beams were also seen. (It appeared that at high exposures, dim replicas of the T and B patterns were superimposed onto the R and L emission.) The lack of emission from the W(110) C facet will be discussed below.

Mass analysis of ions desorbing from the vicinal facets in directions close to normal revealed that O^+ was the only ion seen from any of the surfaces in agreement with previous ESD studies of oxygen on tungsten[10-14].

The O^+ ion yield in the direction normal to the (110) terraces is plotted as a function of oxygen exposure for the R and L terraces in Fig. 7. These direct tracings of recorder plots of the QMS mass 16 output were made for V_e = 120 eV, $I_e \simeq 1 \times 10^{-7}$ A. The "threshold" exposure for O^+ emission normal to each surface corresponds to an oxygen coverage of the order of 0.45 monolayers. Thus, the normal O^+ emission begins after the p(2 x 1) overlayer is well-formed on the terraces. However, the visual evidence indicates that the thresholds for off-normal emission are at lower coverages than for normal emission. Similar threshold results were found for emission normal to the T and B facets.

Ion emission from the W(110) C facet is, at most, very weak. At 4L, a very dim normal beam was seen as the electron beam was scanned over parts of the central (110) facet, with no emission at all

from most of it. At 40L exposure, there were some regions of the central (110) facet where a dim "superposition" pattern appeared, containing a central beam and 6 outer beams (all the beams of Fig. 6). Presumably, this was due to defect structures on the surface. It appears that a perfect W(110) surface gives rise to little or no O^+ ion emission for oxygen coverages $\lesssim$ 0.5 monolayers.

Fig. 8 is a plot of O^+ ion yield normal to (110) terraces as a function of distance along a horizontal line parallel to the central (110) facet, as shown in the inset. The crystal was rotated to face the QMS, and the electron gun was focussed so as to maximize the O^+ ion current from the L facet. Then, the crystal was simply translated along a line perpendicular to the QMS axis without changing the electron beam focus. The point-by-point ion yield was measured as a function of the crystal position and plotted in Fig. 8 for oxygen adsorption at both 340K and 100K (4L exposure). At 340K, the O^+ ion yield from the center of the W(110) facet is only 0.01 times the maximum ion current from the L facet. (Following a 40L O_2 dose, this ratio rises to 0.03). Also, the maximum ion yield from the L facet is consistently higher than that from the R facet. The step density is higher on L than on R, and at constant exposure, the oxygen coverage is also higher (cf. Fig. 4).

Following adsorption at 100K, the O^+ yield from the central W(110) facet is a bit higher relative to R and L, but the absolute intensity of the normal emission from the R and L facets at 100K is about 5 times less intense than for the 300K adsorption. Also, the oxygen coverage on the

central (110) is higher at 100K than at 340K (compare Figs. 4 and 5). Furthermore, when the crystal is heated to 300K following adsorption at 100K, emission from the W(110) C facet disappears with no apparent change in oxygen coverage. (This will be discussed in more detail below.) It thus appears that the low O^+ emission from the central (110) flat at 300K, relative to the vicinal surfaces, is <u>not</u> simply related to the low coverage achievable ($\sim$ 0.5 monolayer) at 300K. The W(110) oxygen coverage is increased to the range 0.6 to 0.7 monolayer by adsorption at 100K (Fig. 5) and yet upon heating to 300K, there is still little or no ion emission. Thus, the low O^+ emission from the central W(110) is <u>not</u> simply related to an oxygen coverage lower than the threshold coverage for ion emission in the normal direction ($\sim$ 0.45 monolayers, cf. Fig. 7). Rather, the presence of a high density of steps on the vicinal surfaces and their absence on the (110) surface appears to be the major factor in the high O^+ yield from the oxygen-covered (110) vicinals.

E. Adsorption of Oxygen at 100K: ESDIAD

When the clean crystal at 100K was exposed to oxygen, small dim ESDIAD patterns containing off-normal beams were observed from the vicinal facets even at exposures of 0.4L (average $\theta \sim 0.2$, cf. Fig. 5). As the coverage increased, the patterns became brighter and more distinct. Fig. 9 contains an array of ESDIAD patterns observed following an oxygen exposure of 4L. The central (110) plane yields a 5-spot pattern having two-fold symmetry (C_{2v}). On T and B facets, an array of downstep beams are seen

in addition to the 5 spot (110) pattern. No less than 11 beams can be clearly seen from the T facet in Fig. 9, with two more weak beams along the [110] azimuth also visible! In contrast, R and L are characterized by extended, non-circular beams.

At all oxygen coverages at 100K only the (1 x 1) LEED pattern was seen on each of the facets; upon heating to less than 300K, ordered patterns characteristic of oxygen adsorption appeared (depending on coverage: p (2 x 1), p(2 x 2)). Upon heating to ∿250K, the ESDIAD patterns from each facet transformed irreversibly into patterns somewhat similar to those of Fig. 6. Neither cooling nor redosing would restore the patterns of Fig. 9. The two-fold pattern of the central (110) disappeared upon heating to ∿250K.

F. ESDIAD of Oxide Layers

When tungsten is heated in oxygen at temperatures $\lesssim$1400K, the growth of tungsten oxide layers occurs[13, 20]. The composition, structure, thickness and kinetics of oxide film formation are dependent upon temperature, gas pressure, and crystal face. It is also well known that heating W in the presence of oxygen can lead to the formation of surface species which desorb with a high O^+ ion yield when studied by electron stimulated desorption (ESD)[9, 13, 20].

In the present case, it is observed that intense ESDIAD patterns are associated with the (110) vicinal facets when their oxide layers are known to be present on the surface. Although no systematic study of the intensity and symmetry of the ESDIAD patterns have been performed, the patterns shown

in Fig. 10 are illustrative of "oxide" patterns. In this case, the crystal was flashed to 2500K, and when the temperature had dropped below ∿1500K, the crystal was exposed to 300L of oxygen as it cooled further. Finally, the sample was heated to ∿900K to remove adsorbed gases and cooled to 100K for the photographs. This treatment is known to produce an oxide layer having a thickness of up to a few monolayers on a polycrystalline W surface[20]. As in the case of the chemisorption structures (Fig. 6 and 9), the ESDIAD patterns are dominated by ion emission normal to the terraces and in the step-down direction. Only O^+ ions are detected, and the symmetry of the pattern is sensitive to the step structure. Ion emission from the W(110) C facet is very weak, with a dim "superposition" pattern seen in some areas. The intense O^+ emission reported by Niehus[21] for ordered WO_3 overlayers on W(110) was not seen in the present case, because the temperature-pressure conditions were not appropriate to form these layers. LEED patterns seen for the (110) surface were similar to those reported by Bauer and Engel[18] for the two dimensional oxidation layer on W(110).

The appearance of the ESDIAD patterns (number of O^+ beams, relative intensities of different O^+ beams) for oxide layers on the multifaceted crystal appears to be a sensitive function of the temperature formation and the total oxygen uptake. The representative patterns of Fig. 10 provide a strong indication that ESDIAD can, when combined with LEED, HEED, etc., be a useful structural tool for oxide surfaces.

The profile of one of the O^+ beams in Fig. 10 is shown in Fig. 11. This is a plot of O^+ ion emission as a function of ion desorption angle, as measured by rotating the crystal about an axis perpendicular to the axis of the quadrupole mass spectrometer. The beam in question is normal to the terrace of the B facet, in the center of the bottom pattern of Fig. 10. The data of Fig. 11 were measured with only a small bias potential (+ 2V) on the sample, so that the ions desorbed in a nearly field-free region, leading to minimal distortion of the ion trajectories[23]. The half width at half maximum (hwhm), α, is 10° at 300K, and decreases to 9° when the sample is cooled to ∿100K. Such a reversible temperature dependence in ESDIAD beam widths has been observed previously[22, 23]. In the case of molecular adsorption (CO on Ru(001)), the temperature dependence of the beam width was associated with the amplitude of surface bending vibrational modes[23]. The relatively small temperature dependence seen in Fig. 11 indicates that the bending frequency (and/or force constant) is higher for tungsten oxide than the low frequency ($\sim$ 85 cm^{-1}) mode responsible for the CO on Ru(001) case. Recent theoretical work[24] predicts bending vibrational amplitudes for surface molecules which are of the order of those deduced from ESDIAD measurements.

IV. Discussion

A. Sticking Probability: Adsorption Kinetics

The study of adsorption kinetics for oxygen on the polyhedral W crystal (Figs. 4, 5, and Table II, as well as Ref. 7) raises some interesting

questions concerning gas-surface processes: Why are the initial sticking probabilities and the saturation coverages higher on the stepped vicinal surfaces than on the flat W(110) surface? Why are the differences in sticking probability and saturation coverage on the different planes much more pronounced at 300K than at 100K? The answers to these questions are directly related to the fundamentals of the oxygen-tungsten interaction.

It has been widely recognized that the maximum coverage easily attainable on W(110) at ~300K is 0.5 monolayers[7, 11, 12, 19] (7.1×10^{14} atoms/cm^2) corresponding to the p(2 x 1) LEED structure. The sticking probability, i.e., the probability for dissociative adsorption of oxygen, decreases precipitously for coverages >0.5 monolayers. In contrast, the sticking probability remains high on the stepped vicinal surfaces for coverages well in excess of 0.5 monolayers.

A qualitative model which appears to be consistent with the observed adsorption kinetics for oxygen at 300K is as follows. An O_2 molecule impinging on a W(110) terrace is adsorbed into a weakly bound molecular precursor state. The following fates are among those possible for the precursor molecule:

(a) If it encounters a pair of bare W sites on the (110) terrace, it can dissociate; the atoms then diffuse to form p (2 x 1) islands.

(b) It can simply desorb from the bare surface, or from the p(2 x 1) oxygen covered surface. (Dissociation atop the p(2 x 1) islands does not occur, although it can occur at the edges.)

(c) It can diffuse over the bare surface or over the p(2 x 1) surface and dissociate; rediffusion of atomic oxygen to a W(110) site leads to filling in of the p(2 x 1) structure, with an increase of oxygen coverage.

The key element in this model is the molecular precursor which can dissociate on the flat (110) terraces, or can diffuse to step sites where dissociation occurs, followed by diffusion of atomic species back out to the terraces. Wang and Gomer[12] have found direct evidence for the presence of a molecular O_2 precursor to chemisorption which is stable in measurable concentrations on a W(110) surface at temperatures $< 50K$. Auerbach et al.[25] have used molecular beam methods to demonstrate that the direct chemisorption of oxygen on polycrystalline W occurs in $\sim 10^{-13}$ sec <u>without</u> a precursor state for $T >> 400K$, but that the adsorption probability is enhanced by the onset of van der Waals trapping into a precursor state below 400K. Thus, the evidence for a mobile molecular precursor in the temperature range of our measurements (100-300K) appears good.

The fact that ordered p(2 x 1) LEED patterns are seen on all facets at 300K is prima facie evidence that at the very least, short range diffusion of atomic oxygen is possible at this temperature. Chen and Gomer[26] have used field emission flicker noise techniques to measure the mobility of oxygen on W(110); they assert that diffusion starts at 450-500K, but that small correlation signals are seen at temperatures as low as 260K. Thus, the idea that atomic oxygen produced by dissociation at step sites can diffuse a few Å over a W(110) terrace at 300K does not appear unreasonable.

Note also that the sticking probabilities (and saturation coverages) for the L facet, with its 13 Å wide terraces, are larger than for the R facet, with its 22 Å wide terraces. This is consistent with short diffusion distances for atomic O. This model differs from that proposed by Gland and Korchak[27] for the adsorption of oxygen on stepped Pt; they presented evidence for rapid adsorption at step sites, followed by adsorption on the terraces without diffusion from step sites to terraces. The present model is similar to that of Singh-Boparai, Bowker and King[28] who discussed nitrogen adsorption on stepped W(110) surfaces. The difference between models is that Singh-Boparai et. al. assumed that dissociation occurs only after diffusion of N_2 to step sites, whereas we believe oxygen dissociates both on (110) terraces and at step sites also.

The p(2 x 1) oxygen structure is not the only W(110) overlayer on which O_2 dissociation does not occur directly. There is good evidence to indicate that O_2 will not dissociatively adsorb on an hydrogen covered W(110) surface[29a] at 300K, nor on a carbide covered W(110) surface. Thus, the necessity of special sites to dissociate oxygen in order to initiate adsorption may be quite general.

Upon adsorption at 100K, the lifetime of the molecular precursor state is longer than at 300K, so diffusion of this species should still occur. However, the fact that no p(2 x 1) LEED pattern is seen at any coverage on any facet indicates that even short-range mobility of adsorbed atomic oxygen is hindered at low temperatures. This implies that step edges do not act as "feeder" sites for atomic oxygen at 100K, and may account for the observation that the differences between the saturation coverages on the various facets is less at 100K than at 300K. In addition, the full monolayer coverage attainable with 20L exposure on the L facet at 300K cannot be achieved at 100K due to the lack of mobility of the adsorbed atomic oxygen.

It is clear from a comparison of Fig. 4 and Fig. 5 that the "saturation" coverage of oxygen on the W(110) flat is higher at 100K than at 300K. Other evidence for enhanced uptake at 100K is the observation of a (2 x 2) LEED pattern upon heating (indicating $\theta > 0.5$[18, 19]). Fuggle and Menzel[29b] used XPS to demonstrate that for exposures equivalent to those employed here, the saturation oxygen coverage on W(110) is ~20% higher at 100K than at 300K. In contrast, the crystal reflection measurements of Wang and Gomer[12] indicated that at both 100K and 300K, the saturation coverage was 0.5 monolayers, although their measurements were not carried to exposures as high as 20 Langmuirs.

There has been some discussion in the literature[7, 17, 18, 29b] concerning the absolute magnitude of the initial sticking probability for the "perfect" W(110) surface at 300K; this has been most recently considered by Fuggle and Menzel[29b]. Our upper limit of 0.38 agrees, to within experimental uncertainty, with the other values (range of 0.28 to 0.5).

We have not yet addressed the issue as to <u>why</u> the step sites promote dissociation and adsorption. Wagner[1] has suggested that step-promoted action localized at step sites may be due to unsaturated bonds or free valence orbitals of edge atoms. Ibach[30] has proposed that the activation barrier for dissociation of adsorbed precursor molecules is lowered by the presence of dipole moments associated with step edges. The present results, as well as previous data[5,7], demonstrate that the geometry of the step edge plays an important role in determining the kinetics of oxygen adsorption; steps parallel to the [111] direction are less "active" than those parallel to [100] or [110]. Much needs to be done theoretically before a detailed

understanding of the role of steps in chemisorption and catalysis is possible.

B. ESDIAD at 300K

At low oxygen coverages (less than a few tenths of a monolayer), there is little or no ion emission from any of the surfaces of the W polyhedron. Only after the p(2 x 1) oxygen structures are reasonably well-developed on each of the facets, then the sites from which the O^+ ion emission originate become populated. Such sites appear to be confined to the stepped vicinal surfaces--there is little or no ion emission from the (110) flat at any coverage for T >300K. The sensitivity of ESDIAD to local step geometry, as seen in the patterns in Fig. 6, suggests that the specific sites responsible for adsorption of the ESD-active species (i.e., the species which give rise to O^+) are located at step edges and defects on the surfaces. We suggest that adsorption of oxygen on low coordination sites, such as those which exist at step edges, kink sites and point defects on close-packed (110) surfaces, are of key importance in ESD of adsorbed oxygen.

The ESDIAD results for chemisorbed oxygen ($T \gtrsim 300K$) and the oxidized surfaces of the polyhedral W crystal are summaried as follows: (a) The only positive ESD ion observed is O^+; (b) The O^+ ESDIAD patterns from the faceted surfaces contain a number of ion beams which depend on step orientation (see Fig. 6); (c) The O^+ ESDIAD patterns from the faceted surfaces are dominated by beams perpendicular to the flats, as well as beams with azimuthal orientation in the step-down directions; (d) A very weak O^+ ESDIAD signal is seen

for oxygen adsorbed on the (110) plane. (e) Intense O^+ emission is observed only after the p(2 x 1) LEED structure is well-developed on the terraces. The results are consistent with an earlier observation of ESD from a stepped surface[14], and suggest that the "ESD-active" sites for O^+ desorption from oxygen or tungsten are low coordination sites which are absent on a perfect (110) surface, but present on the stepped surfaces.

Two possible explanations can be offered to explain this sensitivity of ESD to atomic adsorption at low coordination sites. First of all, on the basis of the one dimensional Redhead-Menzel-Gomer[31, 32] model of ESD, the probability of ionic desorption P_I is exponentially related to the neutralization rate for an ion formed at the surface by electron bombardment, viz.,

$$P_I = \exp\left\{-\int_{x_0}^{\infty} \frac{R(x)}{v(x)}\, dx\right\}$$

where $R(x)$ is the neutralization rate (sec^{-1}), $v(x)$ is the ionic velocity in the repulsive final state, x is the distance from the surface, and x_0 is the separation between atom and surface at the point of excitation. $R(x)$ is a measure of the rate of electron transfer (e.g., tunneling, Auger neutralization) from the substrate to the ion created by electron bombardment, and it is reasonable to assume that $R(x)$ is different for adatoms bonded in different sites. Oxygen atoms adsorbed on W(110) flats are located in multiply-coordinated sites, bonded to 2 or 3 substrate W atoms[33,34]; oxygen atoms adsorbed at step edges may be in atop sites, bonded to single W atoms. An increase in coordination (i.e., the "number of bonds" to the substrate) should result in an increase in $R(x)$ at that site. Since P_I is exponentially dependent on $R(x)$,

even small changes in its value will have a strong influence on ESD ion yield, P_I.

For example, the value of P_I for the high O^+ yielding β_1 oxygen state on polycrystalline W[9,35] is $P_I \sim 3.8 \times 10^{-4}$. This value is approximately correct for ESD of O^+ from stepped W(110) vicinal surfaces; an increase in R(x) by a multiplicative factor of 2 (due to increased coordination of an O atom to the W substrate) will cause a decrease in P_I to 1.4×10^{-7}, more than three orders of magnitude! Thus, the increased O^+ ion yield observed for oxygen adsorbed at step sites is consistent with the expected single coordination of oxygen atoms adsorbed atop single substrate atoms at step edges. Adsorption at "notch" sites at step edges, i.e., sites of high coordination, would be expected to result in a low O^+ ion yield due to increased reneutralization rate. (Note that this argument based on the one dimensional RMG model ignores variations in v and x_o, both of which can also affect P_I). A simple picture which assumes oxygen adsorption on the unreconstructed surface, and which yields O^+ desorption in directions appropriate to 300K oxygen adsorption (Fig. 6) is shown in Fig. 12. Multiply-coordinated O in the p(2 x 1) structure does <u>not</u> yield O^+.

Recently, Knotek and Feibelman[36] have proposed that many ESD processes occur via an interatomic Auger decay model. They suggest that Auger decay of core holes produced by electron bombardment of the surface of an oxide explains both the observed thresholds[36] and the large charge transfer (2 or 3 electrons) involved in ESD of O^+ from maximal valency metal oxides. The mechanism is expected to be applicable for oxides in which there are no

valence electrons on the metal atom (e.g., WO_3). Engel and coworkers[11] have previously suggested that ESD of O^+ from oxygen on tungsten is related to the formation of oxide-like molecular complexes on the surface. A possible interpretation of the enhanced O^+ emission from step edges may involve the formation of oxide-like complexes at step sites, with the enhanced O^+ yield due to the Auger decay mechanism. A final resolution of the details of ESD processes at step edges must await careful threshold measurements, as well as measurements of the energy distributions of ions desorbing in different directions.

If we accept the fact that special sites atop step edges are responsible for the ESDIAD patterns, we must ask whether or not all sites at step edges are "ESD-active", or whether the oxygen which desorbs as O^+ is adsorbed in just a few special sites. A corollary to this question is: are the oxygen adsorption sites atop the unreconstructed step edge (as shown in Fig. 12), or is the step reconstructed upon adsorption of oxygen? An estimate of the actual concentration of "ESD-active" species would be of use in answering these questions.

Engel et al.[11] found for oxygen adsorption on their W(110) crystal that the concentration of ESD active species, relative to the inactive species, is less than 4%. That is, >96% of the oxygen adsorbed did not contribute to the O^+ ESD ion yield. Similar conclusions have been drawn for polycrystalline W[9]. In the present case, we have compared the decrease in O^+ ion yield on the L and R facets with the intensity of the O(KVV) AES signal as a function of electron bombardment dose for a 4L O_2 dose. In the time that it takes for the O^+ yield to drop to $^1/_e$ of its initial value, the O(KVV) signal has decreased by (at most) a few percent! We cannot be sure that the decrease in O^+ is due entirely to desorption; perhaps an electron stimulated conversion of the adsorbed oxygen to an ESD-inactive

state occurs (e.g., from an atop site to a notch site). By analogy, Naumovets and Fedorus[37] have observed an electron bombardment-induced disordering in adsorbed H and Li on W(110). The fact that gentle heating to $\gtrsim$500K causes the patterns of Fig. 6 to disappear without apparent desorption suggests that, in the present case, such conversions can be induced thermally; a similar observation was made by Steinbruchel and Gomer.[38] In any event, the results are not conclusive. A lower limit on the concentration of ESD-active species, as indicated by the AES results, is a few percent. A reasonable upper limit on the concentration of ESD-active species is the ratio of edge atoms to terrace atoms (1/6 and 1/10 for L and R facets, respectively).

It should be noted that there is both experimental[39] and theoretical[40] evidence to suggest that kink-free steps oriented in low index directions are not thermodynamically stable, and that they reconstruct upon heating to include kinks. The kink density will clearly be smaller than the density of step edge atoms, and these may be the sites at which the ESD-active species adsorb.

In summary, for O_2 adsorption at $\sim$300K on vicinal W(110) surfaces, there is little or no ESD O^+ ion desorption at oxygen coverages below $\sim$0.3-0.45 monolayers during which time the p(2 x 1) structure is well developed. For higher oxygen coverages, adsorption of oxygen atop substrate atoms at step sites becomes energetically favorable, and these are the sites from which the O^+ ESD emission originates. For the "perfect" W(110) surface, there is little or no O^+ ion emission even for $\theta \gtrsim 0.6$ monolayers. Previous reports[11,12] of O^+ from W(110) at T $\gtrsim$300K were probably due to adsorption at steps and defects.

C. ESDIAD at 100K

When oxygen is adsorbed at 100K, the LEED patterns remain (1 x 1) for all surfaces, and the p(2 x 1) LEED patterns appear only upon heating to

T <300K. Thus, mobility of the chemisorbed O atoms is hindered to the extent that p(2 x 1) islands do not form at low temperatures. Despite this lack of mobility of the chemisorbed species, the ESDIAD patterns (Fig. 9) show clear evidence for structures in distinct registry with the substrate. As has been mentioned previously[14,41], ESDIAD is sensitive to the local bonding geometry; as long as the local molecular configurations have well-defined azimuthal and polar registry with the substrate, long-range two dimensional order in the overlayer is not necessary to produce an ESDIAD pattern with directed ion beams.

As the surface is heated, the ESDIAD patterns of Fig. 9 convert irreversibly to patterns resembling Fig. 6, at a temperature slightly below the LEED-ordering temperature. Thus the Fig. 9 ESDIAD patterns represent "metastable" configuations which precede the formation of strong chemisorption bonds. The possible configurations in this metastable state are many and complex, as indicated by the multiplicity of ion beams from the T and B facets, Fig. 9. Although a specific model of the oxygen structures is not proposed, several specific conclusions regarding these configurations can be drawn, as discussed below.

Unlike the case of 300K adsorption, a symmetric C_{2v} ESDIAD pattern is seen from the oxygen-covered W(110) plane at 100K (Fig. 9). This pattern, apparently associated with the flat W(110) terraces, is also seen as contributing to the ESDIAD emission from the T and B facets, but is absent in the R and L emission. These observations raise two questions: why is any ESD pattern observed from the (110) flat, and why does the structure of neighboring steps influence the ESDIAD pattern from terraces having (110) orientation?

Although no O^+ ion emission is observed from the chemisorbed oxygen on a (110) flat at 300K, perhaps some of the oxygen is adsorbed in singly coordinated atop sites, or as a molecular species on this surface at 100K. There is no evidence for a high concentration of molecular species on W(110) at 100K; Gomer[12] asserts that molecular oxygen desorbs below 50K. However, the possibility of a low concentration of strongly bound molecular species which converts to chemisorbed atomic oxygen upon heating cannot be eliminated (particularly if the low concentration of molecules or atoms in low-coordination sites have a high ESD cross section).

Finally, the influence of the steps on emission from the terrace at 100K may be a consequence of short-range mobility of the weakly-bound molecular precursor to chemisorption. The structure of oxygen adsorbed at the step edge may "propagate" across the (110) terraces as oxygen coverage increases on the R and L facts, preventing the formation of the structure which forms on C, T and B.

V. Epilogue

It is clear that the presence of atomic steps on W(110) surfaces has a profound influence on oxygen adsorption kinetics, surface molecular structure, and electron stimulated desorption of O^+. Many unanswered questions remain: What is the atomic structure of the steps, are they reconstructed, what is their influence on molecular (non-dissociative) adsorption?

Finally, the question arises: are all phenomena involving ESD of ions associated with adsorption at "special" sites like steps, defects, etc? The answer, in general, is "No." The case of molecular adsorption is most clear. When the ESD process involves breaking an internal molecular bond[23,41] (the C...O bond in absorbed CO, the C...H bond in adsorbed C_6H_{12}, the H...O bond in adsorbed H_2O, etc.), the ionic ESD signal arises from species adsorbed on flats, as well as other sites. Of course, the presence of steps can lead to "inclined" molecules (e.g., CO) but the species on the flats are visible as well.[42, 43] Much more must be done to completely clarify the role of steps and defects in ESD of dissociatively adsorbed species other than oxygen. Finally, the role of steps in ESD of neutrals is an unexplored area.

VI. Acknowledgements

The author is particularly grateful to K. Besocke (Jülich) for the polyhedral W crystal, and to Mr. A. Pararas for his assistance in mounting the crystal. Valuable discussions were held with K. Besocke and H. Wagner, as well as J. T. Yates, Jr., T.-M. Lu and G.-C. Wang. This work was supported in part by the U.S. Office of Naval Research.

Table I

Characteristics of facets on polyhedral W crystal

Facet Designation	Orientation	Deviation from (110) surface	Step parallel to	Terrace Width (Å)	Step density(10^6/cm)
C (center)	W(110)	0^{+}_{-} 0.3°			0^{+}_{-} 0.3
R (right)	W(S)-[10(110)x(1$\bar{1}$0)]	$5.9^{+}_{-}0.5°$	[100]	22	$4.6^{+}_{-}0.4$
L (left)	W(S)-[6(110)x(1$\bar{1}$0)]	$9.9^{+}_{-}0.5°$	[100]	13	$7.7^{+}_{-}0.4$
T (top)	W(S)-[15(110)x(112)]	$5.5^{+}_{-}0.5°$	[110]	23	$4.3^{+}_{-}0.4$
B (bottom)	W(S)-[8(110)x(112)]	$9.7^{+}_{-}0.5°$	[110]	13	$7.5^{+}_{-}0.4$

Table II

Relative Initial Sticking Probabilities s/s_{max} for Oxygen on Polyhedral W Crystal at T ~300K: Comparison with Ref. 7.

Facet Designation	Orientation	s/s_{max} (present work)	s/s_{max} for corresponding facet in Ref. 7
C	W(110)	0.38	0.28
R	W(S)-[10(110)x(1$\bar{1}$0)]	0.79	0.65
L	W(S)-[6(110)x(1$\bar{1}$0)	1.0	1.0
T	W(S)-[15(110)x(112)]	1.0	0.53
B	W(S)-[8(110)x(112)]	0.97	0.8

FIGURE CAPTIONS

Figure 1 Schematic drawing of the polyhedral tungsten crystal used in this work.

Figure 2 Drawing of ideal, unreconstructed tungsten (110) crystal surface showing the atomic structure of steps parallel to [100] and [110] directions. This model is oriented in the same way as the following LEED and ESDIAD patterns.

Figure 3 LEED patterns characteristic of clean facets of polyhedral W crystal. Electron energy = 110 eV, angle of incidence ~40°. To photograph the different patterns, either the beam was moved using deflection plates, or the sample was moved.

Figure 4 Normalized O(KVV) peak-to-peak Auger signal as a function of oxygen exposure for each of the W facets. All data are for a single exposure run. $T_{ads} \simeq$ 340K. As described in the text, the ordinate scale corresponds to the oxygen coverage in monolayers.

Figure 5 Normalized O(KVV) peak-to-peak Auger signal as a function of oxygen exposure, $T_{ads} \simeq$ 100K.

Figure 6 ESDIAD patterns for adsorption of oxygen on multifaceted tungsten crystal, 4 L exposure, $T_{ads} \simeq$ 300K. The center of each pattern corresponds to the normal to the (110) terrace. Top pattern is from the T facet, bottom pattern is from B facet, etc. Electron energy = 300 V.

Figure 7 Normalized ESD O^+ ion yield normal to the (110) terraces as a function of oxygen exposure for the R and L facets. $T_{ads} \simeq$ 340K, V_e = 120 V.

Figure 8 Normalized ESD O^+ ion yield normal to (110) terraces as a function of distance in [110] direction. $T_{ads} \simeq$ 100K and 340K, respectively.

Figure 9 ESDIAD patterns for adsorption of oxygen on multifaceted tungsten crystal, 4 L exposure, $T_{ads} \simeq$ 100K. Electron energy $\simeq$ 300 eV.

Figure 10 ESDIAD patterns for thin oxide layer on multifaceted W crystal.

Figure 11 Reversible temperature effect in ESDIAD. Profile of O^+ ion beam (normal to 110) terrace of the B facet, cf. Fig 10): intensity of O^+ signal as a function of ion desorption angle for T = 300K and 100K.

Figure 12 Schematic model for oxygen adsorption on W(110) flat and step edges. Sites 1 are the triply coordinated sites for the p(2 x 1) LEED structure. Sites 2 give rise to normal O^+ emission from the step edges. Sites 3, 3' and 4 are envisioned as the source of off-normal emission (cf. Fig. 6).

REFERENCES

1. For a comprehensive review, see H. Wagner, Physical and Chemical Properties of Stepped Surfaces, Springer Tracts of Modern Physics (1978).
2. M. Henzler, Appl. Phys. 9, 11 (1976).
3. C. S. McKee, M. W. Roberts, and M. L. Williams, Adv. Coll. and Interface Sci. 8, 29 (1977).
4. K. Besocke and H. Wagner, Surface Science 52, 653 (1975).
5. T. Engel, T. von dem Hagen, and E. Bauer, Surface Sci. 62, 361 (1977).
6. B. Krahl-Urban, E. A. Niekisch, and H. Wagner, Surface Sci. 64, 52 (1977).
7. K. Besocke and S. Berger in R. Dobrozemsky et. al., ed., Proc. 7th Intern. Vac. Congr. and 3rd Intern. Conf. Solid Surfaces, Vienna, 1977 (R. Dobrozemsky et. al., publ.) p. 893.
8. K. Besocke and H. Wagner, 38th Physical Electronics Conference, Gatlinburg, Tennessee, June 1978.
9. T. E. Madey and J. T. Yates, Jr., Surface Sci. 11, 327 (1968).
10. T. E. Madey, Surface Sci. 33, 355 (1972).
11. T. Engel, H. Niehus and E. Bauer, Surface Sci. 52, 237 (1975).
12. C. Leung, Ch. Steinbrüchel, and R. Gomer, Appl. Phys. 14, 79 (1977); C. Wang and R. Gomer, Surface Science 74, 389 (1978).
13. V. N. Ageev and N. I. Ionov, in Progress in Surface Science, S. G. Davison, ed., 5, 1 (1975) [Pergamon Press, New York].
14. T. E. Madey and J. T. Yates, Jr., Surface Science 63, 203 (1977).
15. The crystal was generously provided to us by K. Besocke, and is similar to the one described in Ref. 7.

16. S. Berger and U. Linke, to be published; E. Preuss, B. Krahl-Urban, R. Butz; Lane Atlas (Vieweg, Wiesbader and Halsted, New York, 1974).

17. B. Lang, R. W. Joyner and G. A. Somorjai, Surface Sci. 30, 440 (1972).

18. E. Bauer and T. Engel, Surface Science 71, 695 (1978).

19. M. G. Lagally, G.-C. Wang, and T.-M. Lu, CRC Reviews of Solid State Sciences, "Chemistry and Physics of Solid Surfaces, Vol. II," p. 153 (R. Vanselow, Ed., 1979).

20. D. A. King, T. E. Madey, and J. T. Yates, Jr., J. Chem. Phys. 55, 3237 (1971); J. Chem. Soc. Faraday Trans. I, 7, 1347 (1972).

21. H. Niehus, Surface Science 78, 667 (1978).

22. T. E. Madey, J. J. Czyzewski, and J. T. Yates, Jr., Surface Science 49, 465 (1975).

23. T. E. Madey, Surface Science 79, 575 (1979).

24. N. V. Richardson and A. M. Bradshaw, Surface Sci, to be published.

25. D. Auerbach, C. Becker, J. Cowin and L. Wharton, Appl. Phys. 14, 411 (1977).

26. J. R. Chen and R. R. Gomer, Surface Science 79, 413 (1979).

27. J. L. Gland and V. Korchak, Surface Sci. 75, 733 (1978).

28. S. P. Singh-Boparai, M. Bowker, and D. A. King, Surface Sci. 53, 55 (1975)

29. a.) M. Steinkilberg and D. Menzel, Prof. 7th Int. Vac. Cong. and 3rd Int. Conf. on Solid Surfaces, R. Dobrozemsky et. al., ed. (Vienna, 1977) p. 1163.

b.) J. C. Fuggle and D. Menzel, Surface Science 79, 1 (1979).

30. H. Ibach, Surface Sci. 53, 444 (1975).

31. P. A. Redhead, Can. J. Phys. 42, 886 (1964).

32. D. Menzel and R. Gomer, J. Chem. Phys. 41, 3311 (1964).

33. J. C. Buchholz, Ph. D. Thesis, U. of Wisconsin, 1974.

34. M. A. van Hove and S. Y. Tong, Phys. Rev. Lett. 35, 1092 (1975).

35. T. E. Madey, J. T. Yates, Jr., D. A. King, and C. J. Uhlaner, J. Chem. Phys. 52, 5215 (1970).

36. M. Knotek and P. J. Feibelman, Phys. Rev. Lett. 40, 964 (1978); P. J. Feibelman and M. L. Knotek, Phys. Rev. B15, 6531 (1978).

37. A. G. Naumovets and A. G. Fedorus, Soviet Physics J.E.T.P. 68, 1183 (1975).

38. Ch. Steinbruchel and R. Gomer, Appl. Phys. 15, 141 (1978).

39. F. Hottier, J. B. Theeten, A. Masson, and J. L. Domange, Surface Sci. 65, 563 (1977).

40. J. P. Hirth, in W. M. Mueller, ed., Energetics in Metallurgical Phenomena, Vol. II (Gordon and Breach, New York, 1965), p. 1.

41. T. E. Madey and J. T. Yates, Jr., Chem. Phys. Lett. 51, 77 (1977); Surface Science 76, 397 (1978).

42. T. E. Madey, J. T. Yates, Jr., A. M. Bradshaw, and F. M. Hoffmann, Surface Science, in press.

43. T. E. Madey, J. E. Houston, and S. C. Dahlberg, to be published.

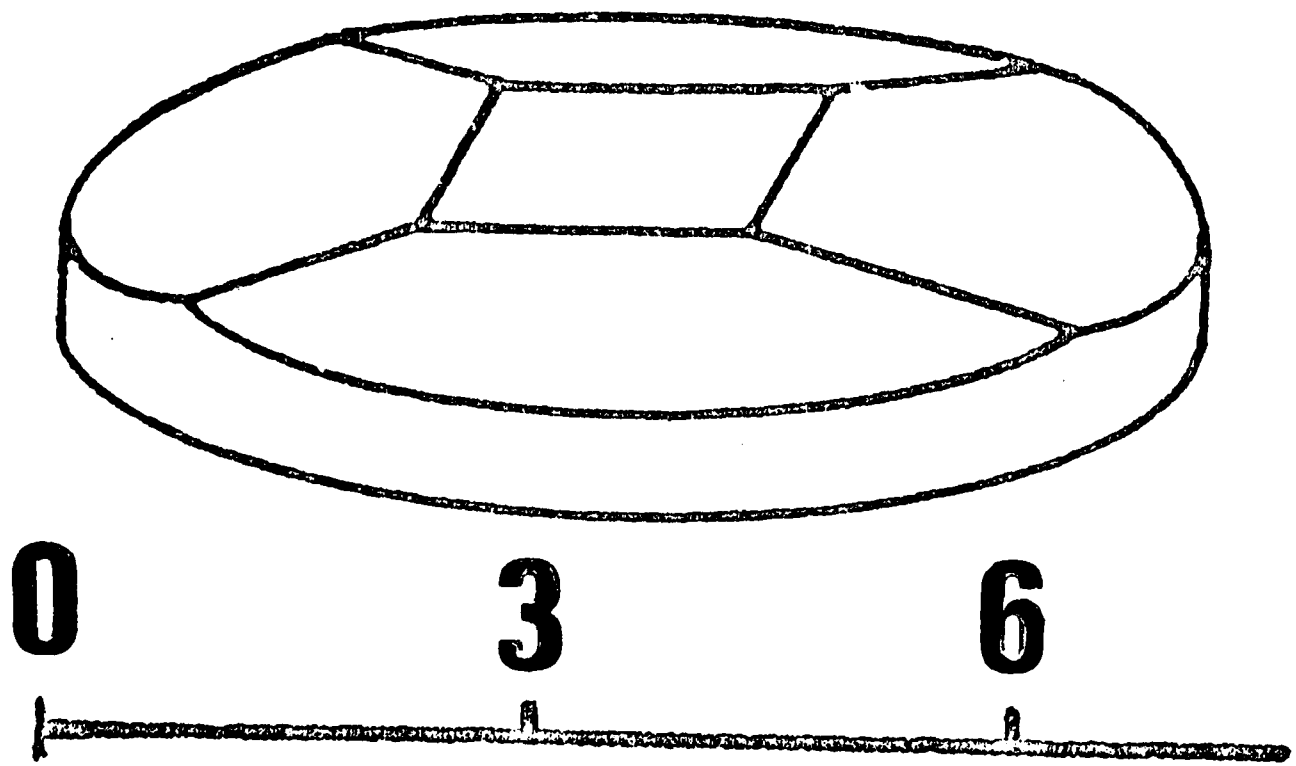
0
3
6
mm

ATOMIC ARRANGEMENT OF W (110) SURFACE SHOWING STEP GEOMETRY

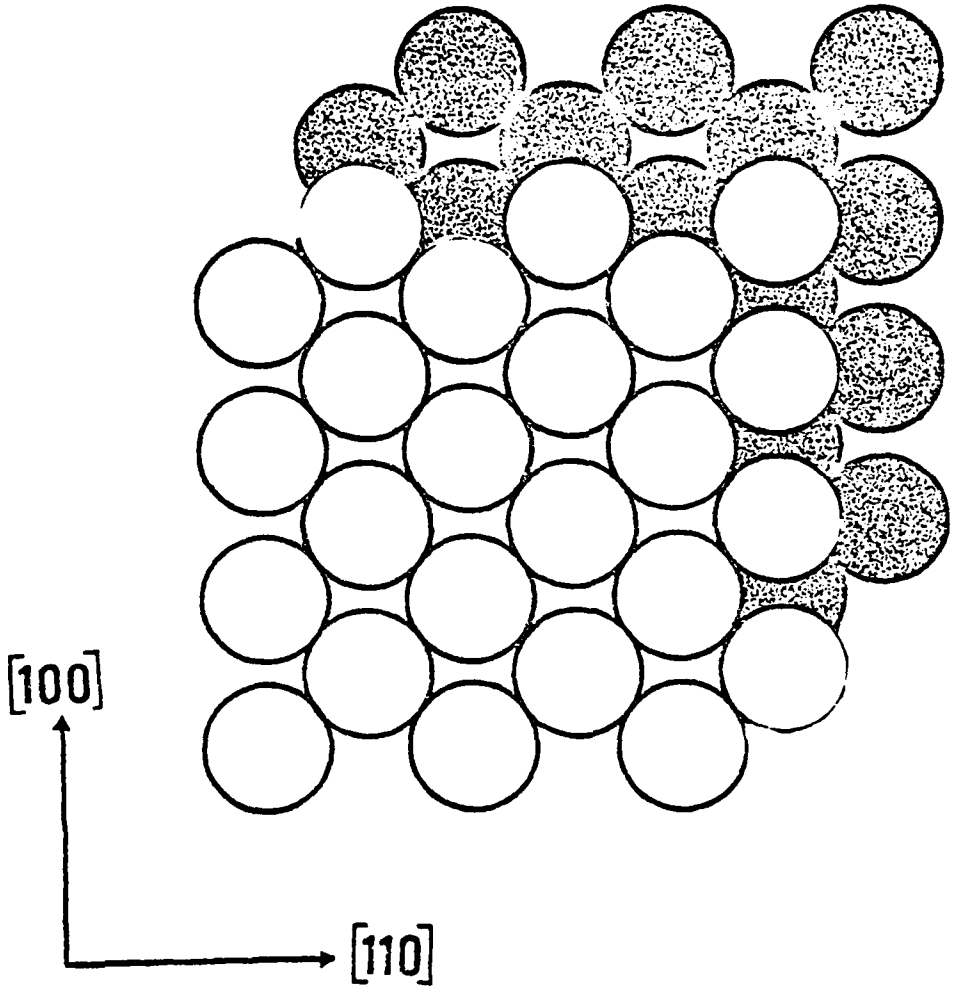

LEED PATTERNS FROM CLEAN MULTIFACETED W (110) CRYSTAL

V_e = 110 V

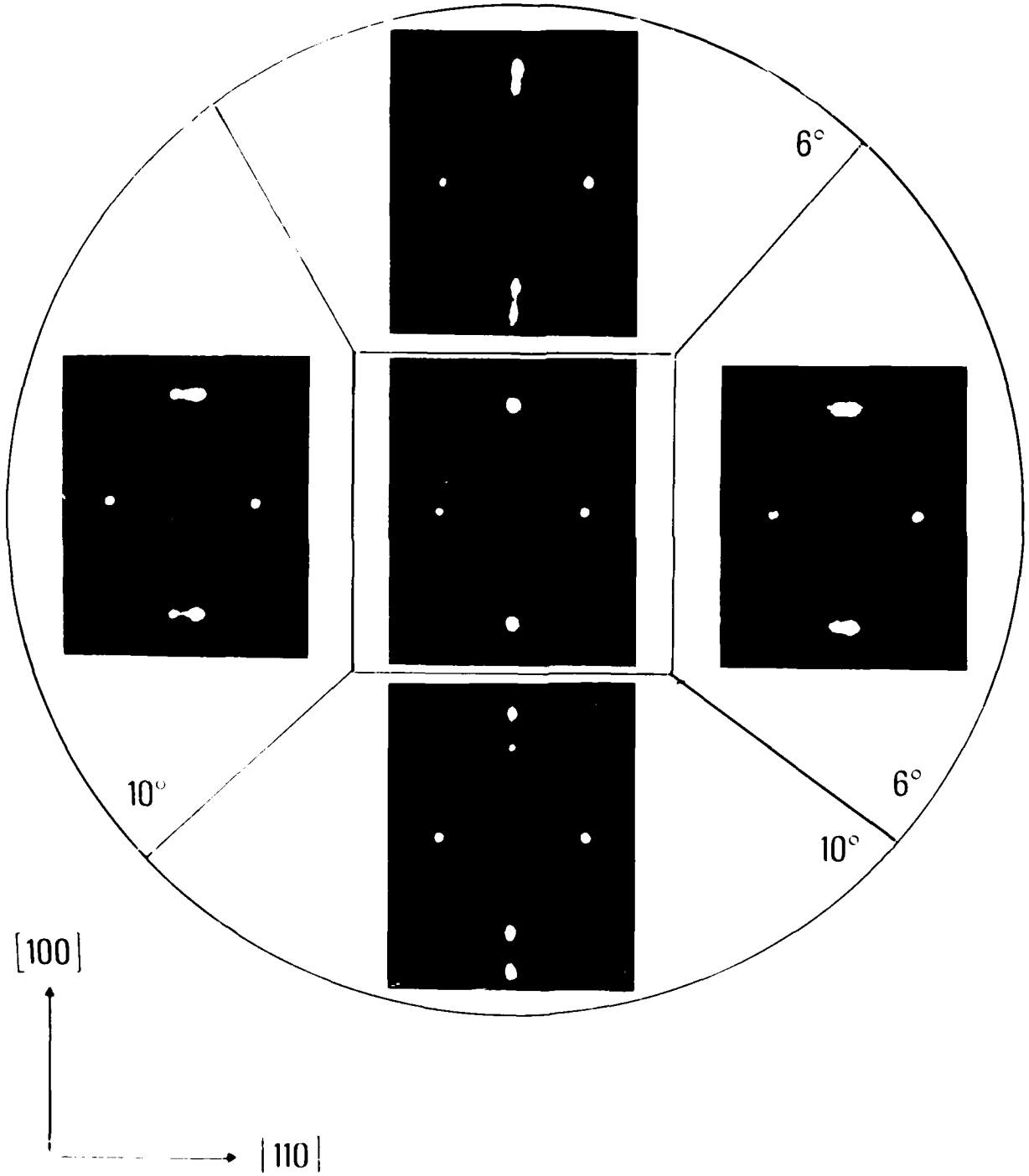

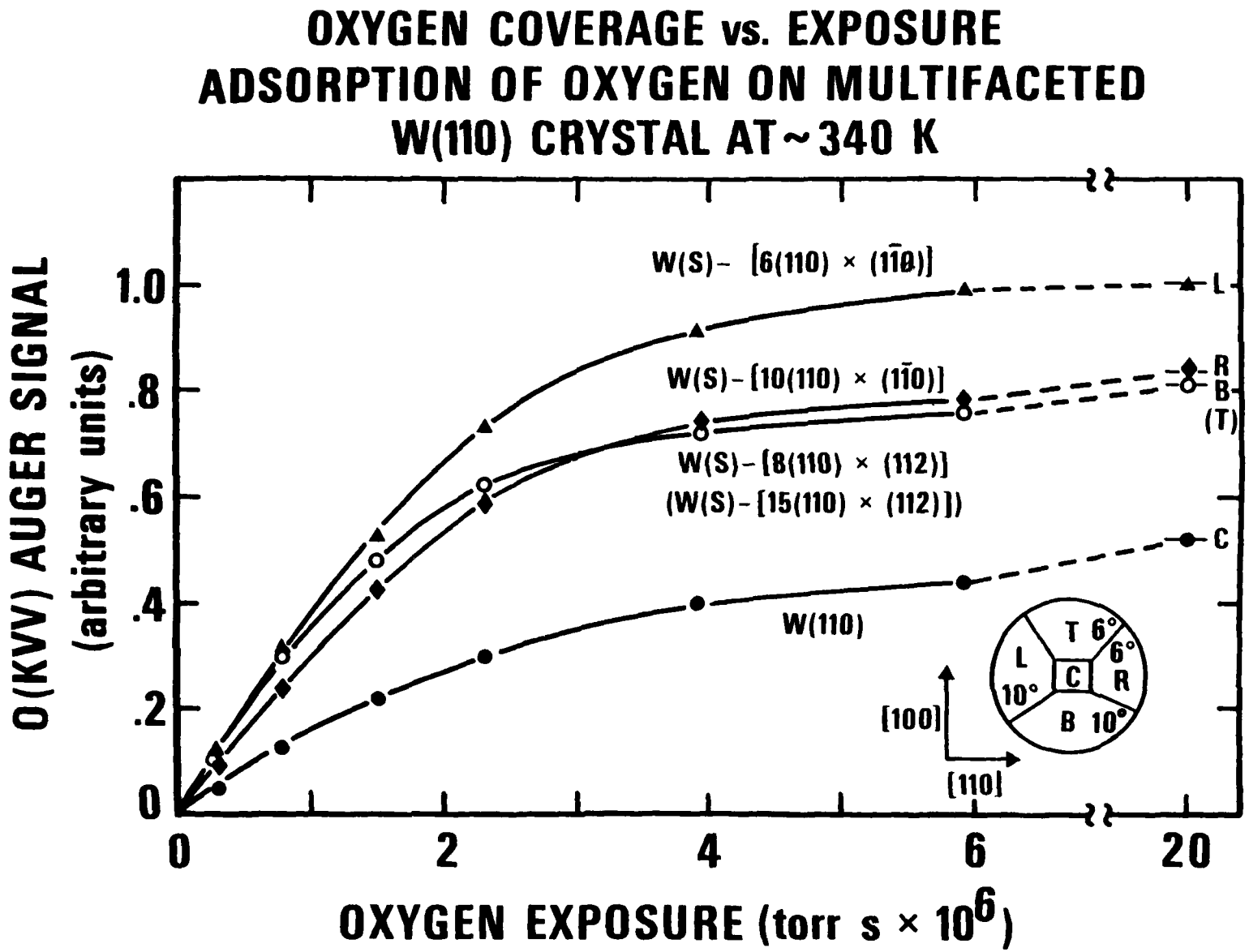
OXYGEN COVERAGE vs. EXPOSURE
ADSORPTION OF OXYGEN ON MULTIFACETED
W(110) CRYSTAL AT ~ 340 K
O(KVV) AUGER SIGNAL
(arbitrary units)
1.0
.8
.6
.4
.2
0
0
2
4
6
20
OXYGEN EXPOSURE (torr s × 10^6)
W(S)- [6(110) × (1$\bar{1}$0)]
W(S)- [10(110) × (1$\bar{1}$0)]
W(S)- [8(110) × (112)]
(W(S)- [15(110) × (112)])
W(110)
L
R
B
(T)
C
T 6°
6°
L
10°
C
R
B 10°
[100]
[110]

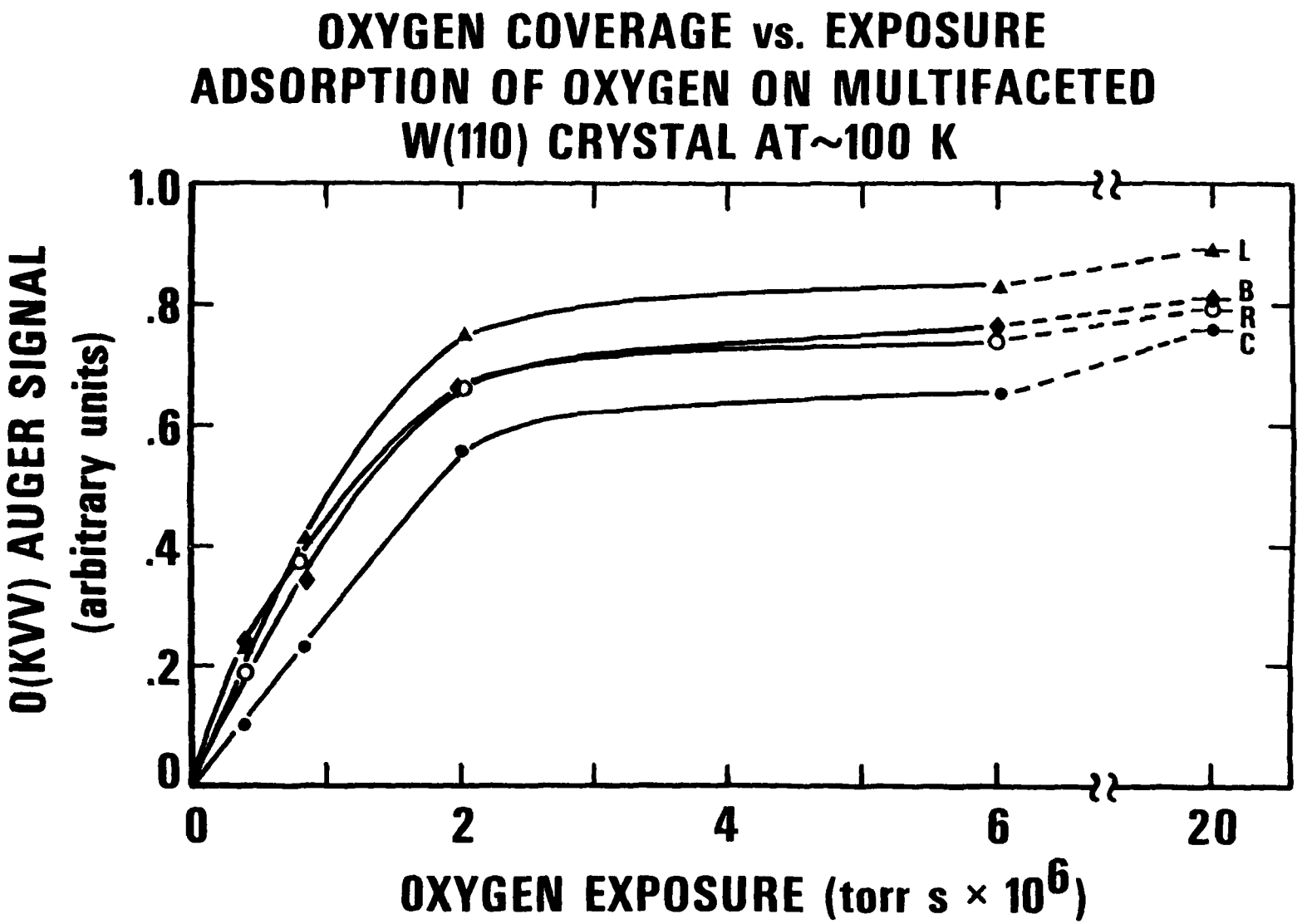
OXYGEN COVERAGE vs. EXPOSURE
ADSORPTION OF OXYGEN ON MULTIFACETED
W(110) CRYSTAL AT~100 K
O(KVV) AUGER SIGNAL
(arbitrary units)
1.0
.8
.6
.4
.2
0
0
2
4
6
20
OXYGEN EXPOSURE (torr s × 10^6)
L
B
R
C

ADSORPTION OF OXYGEN ON MULTIFACETED W(110) CRYSTAL AT~ 340 K EXPOSURE≃ 4 LANGMUIRS

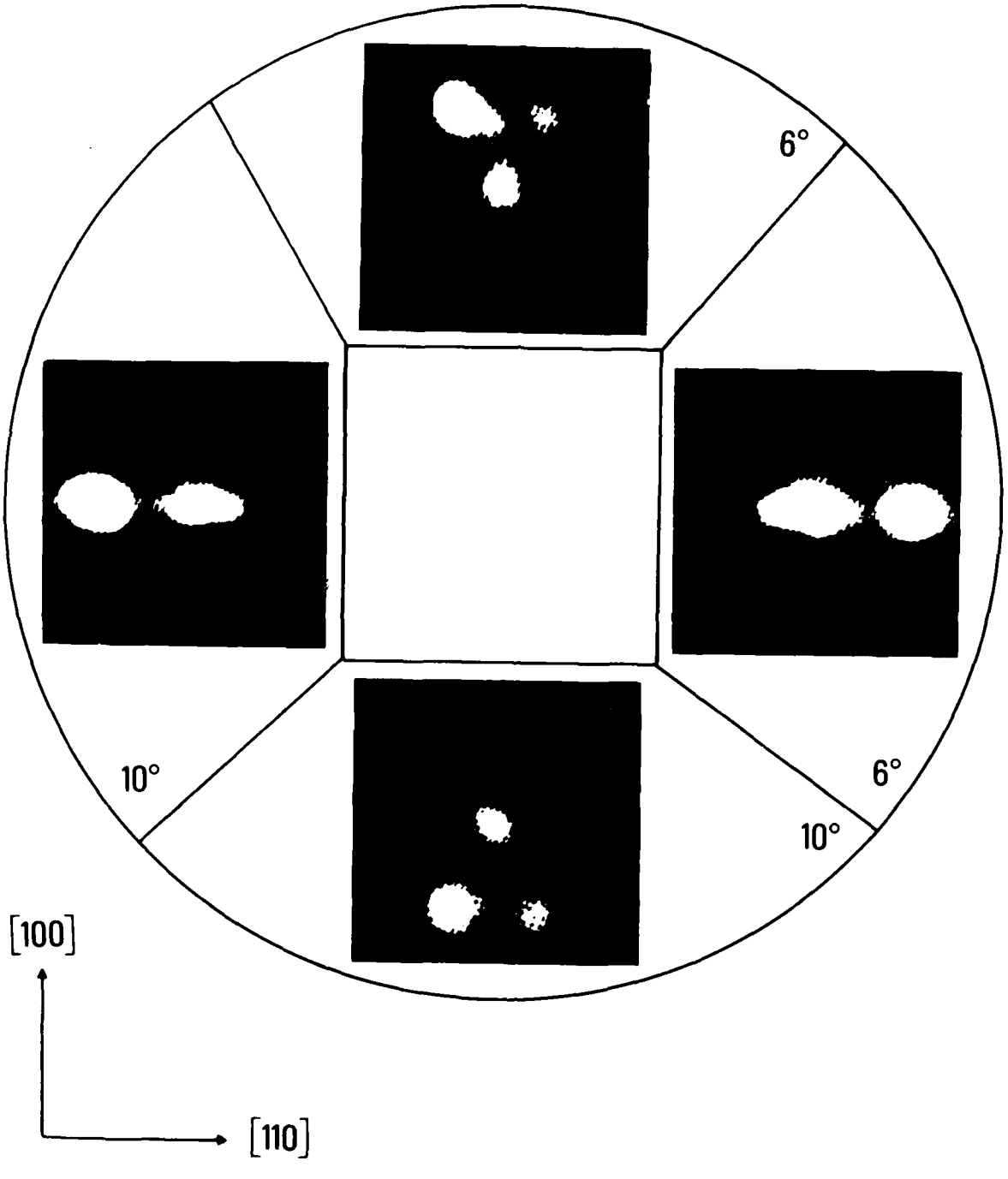

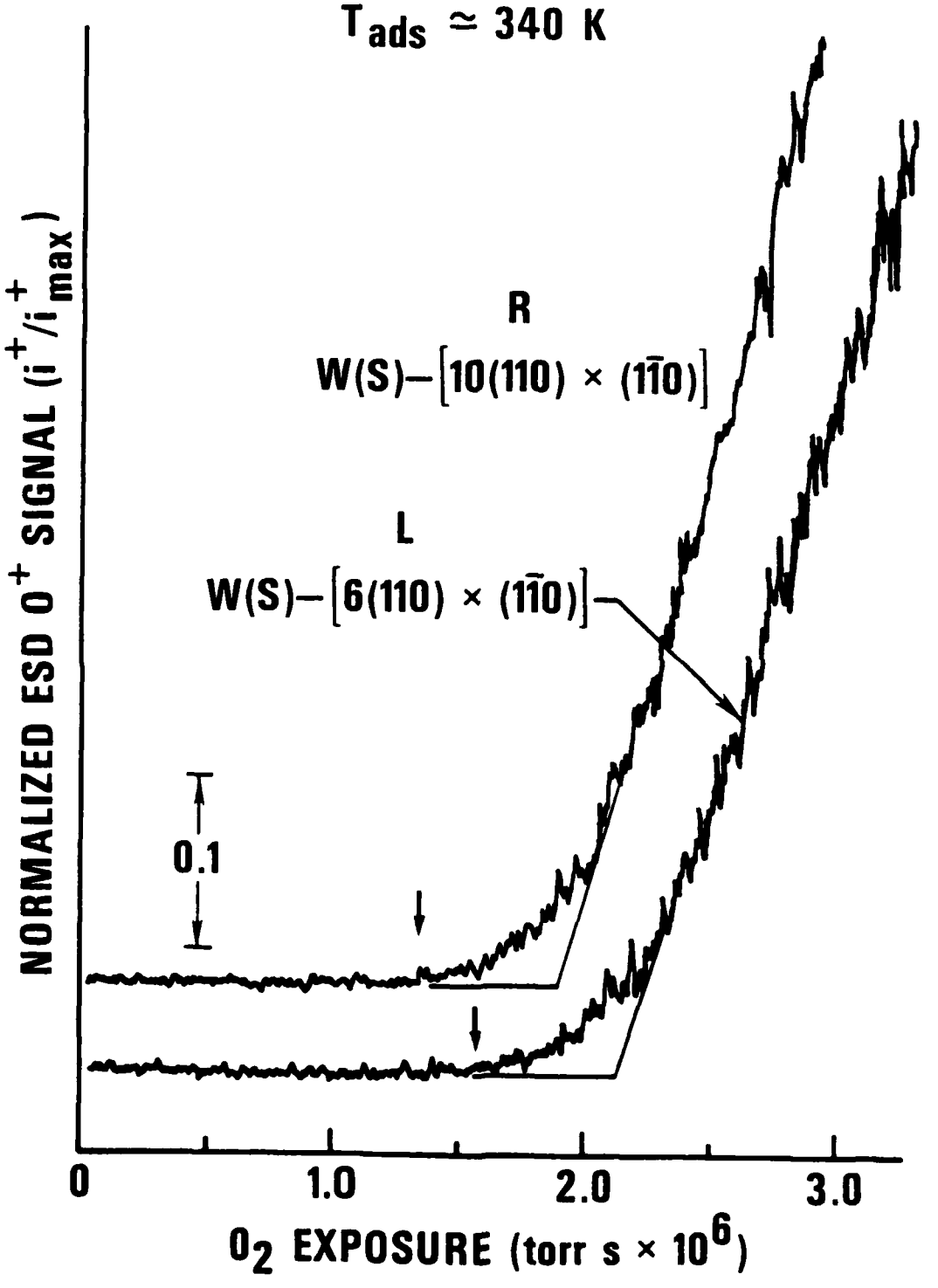
ESD O^+ YIELD vs. OXYGEN EXPOSURE
ON MULTIFACETED W CRYSTAL
$T_{ads} \simeq 340$ K
R
W(S)–[10(110) × (1$\bar{1}$0)]
L
W(S)–[6(110) × (1$\bar{1}$0)]
0.1
NORMALIZED ESD O^+ SIGNAL (i^+/i^+_{max})
0
1.0
2.0
3.0
O_2 EXPOSURE (torr s × 10^6)

INTENSITY OF O^+ ION YIELD NORMAL TO (110) SURFACE, AS A FUNCTION OF DISTANCE IN [110] DIRECTION (4 L DOSE OF O_2)

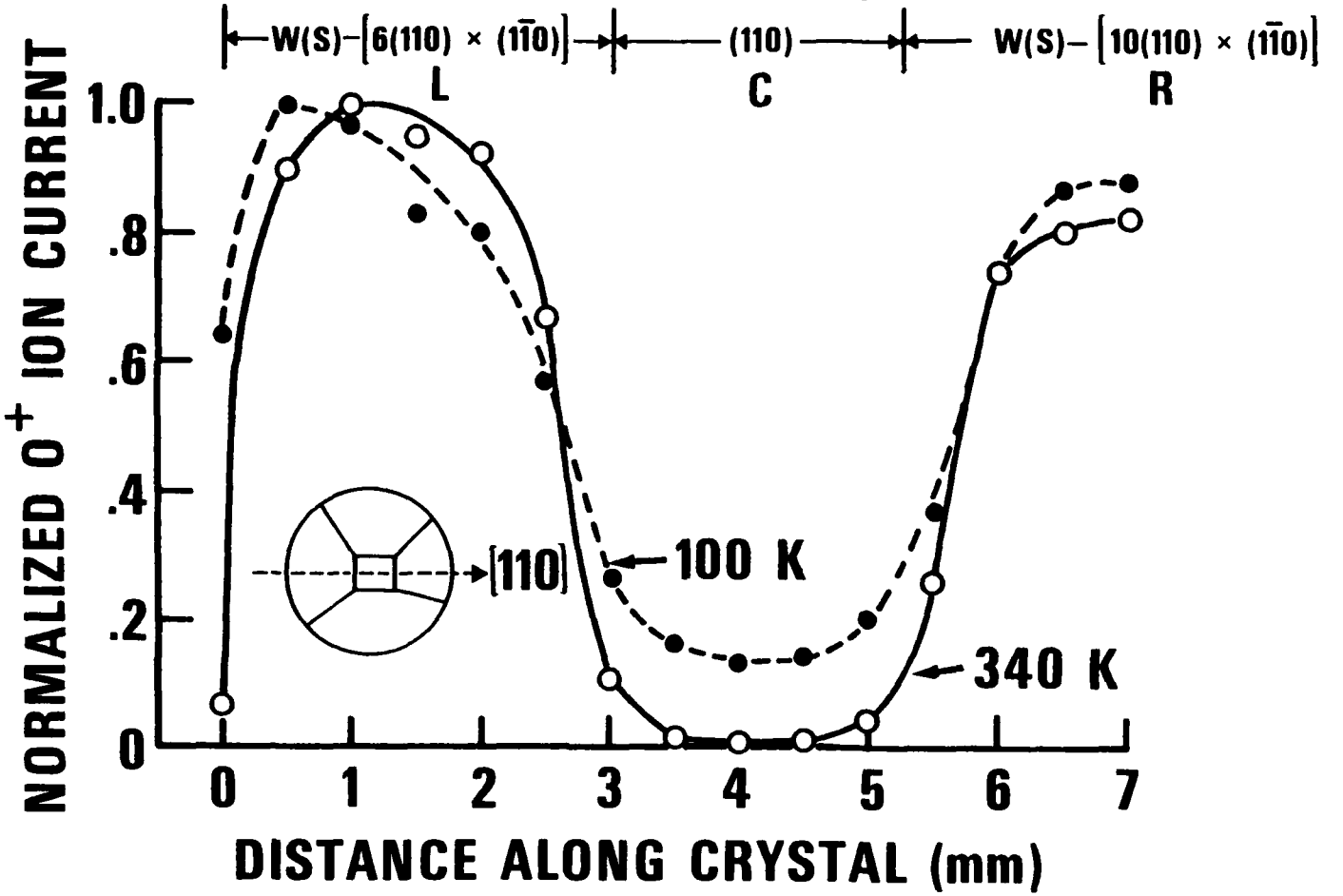

ADSORPTION OF OXYGEN ON MULTIFACETED W(110) CRYSTAL AT ~ 100 K EXPOSURE = 4 LANGMUIRS

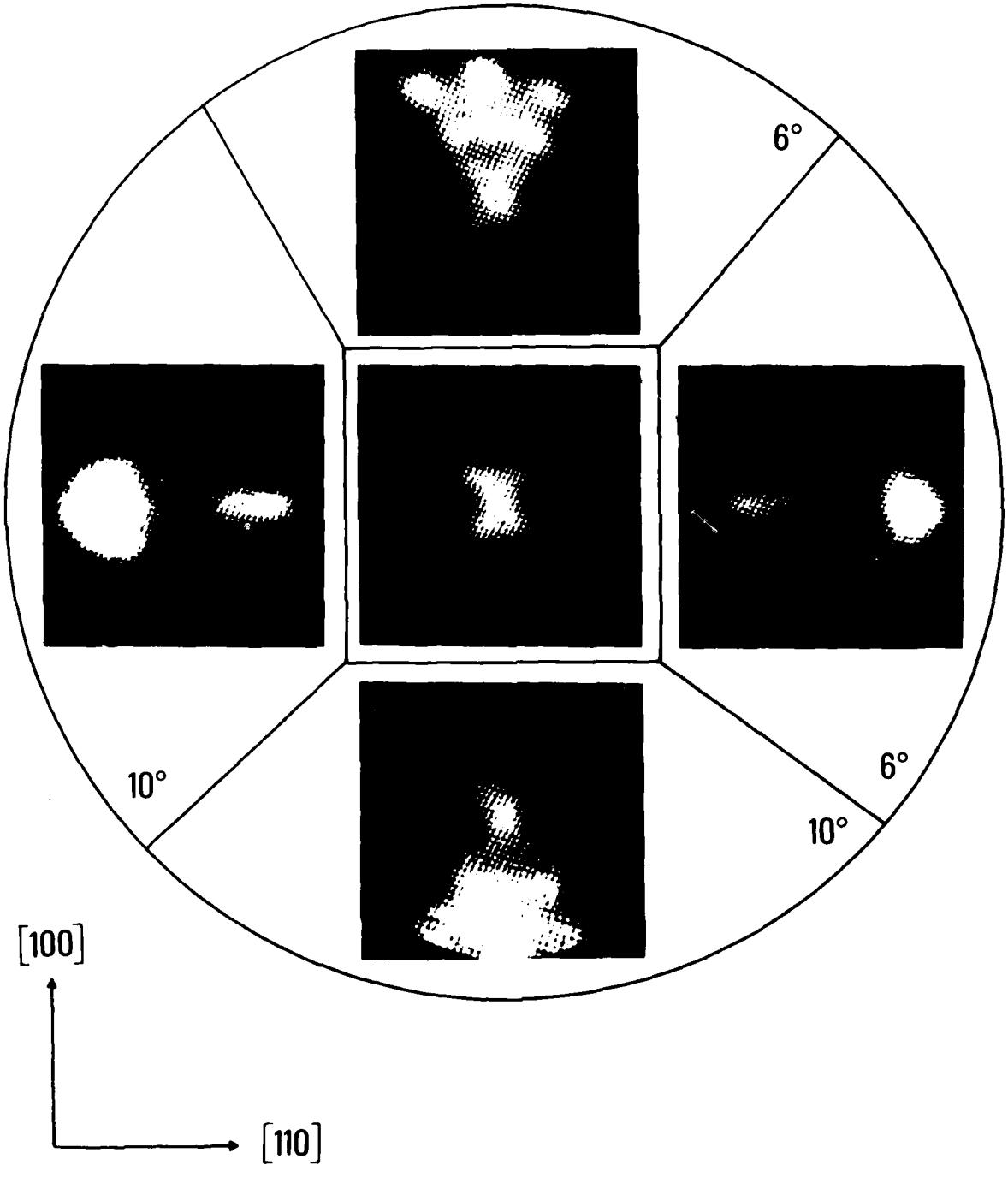

ESDIAD PATTERNS FOR OXIDIZED, FACETED W (110) CRYSTAL

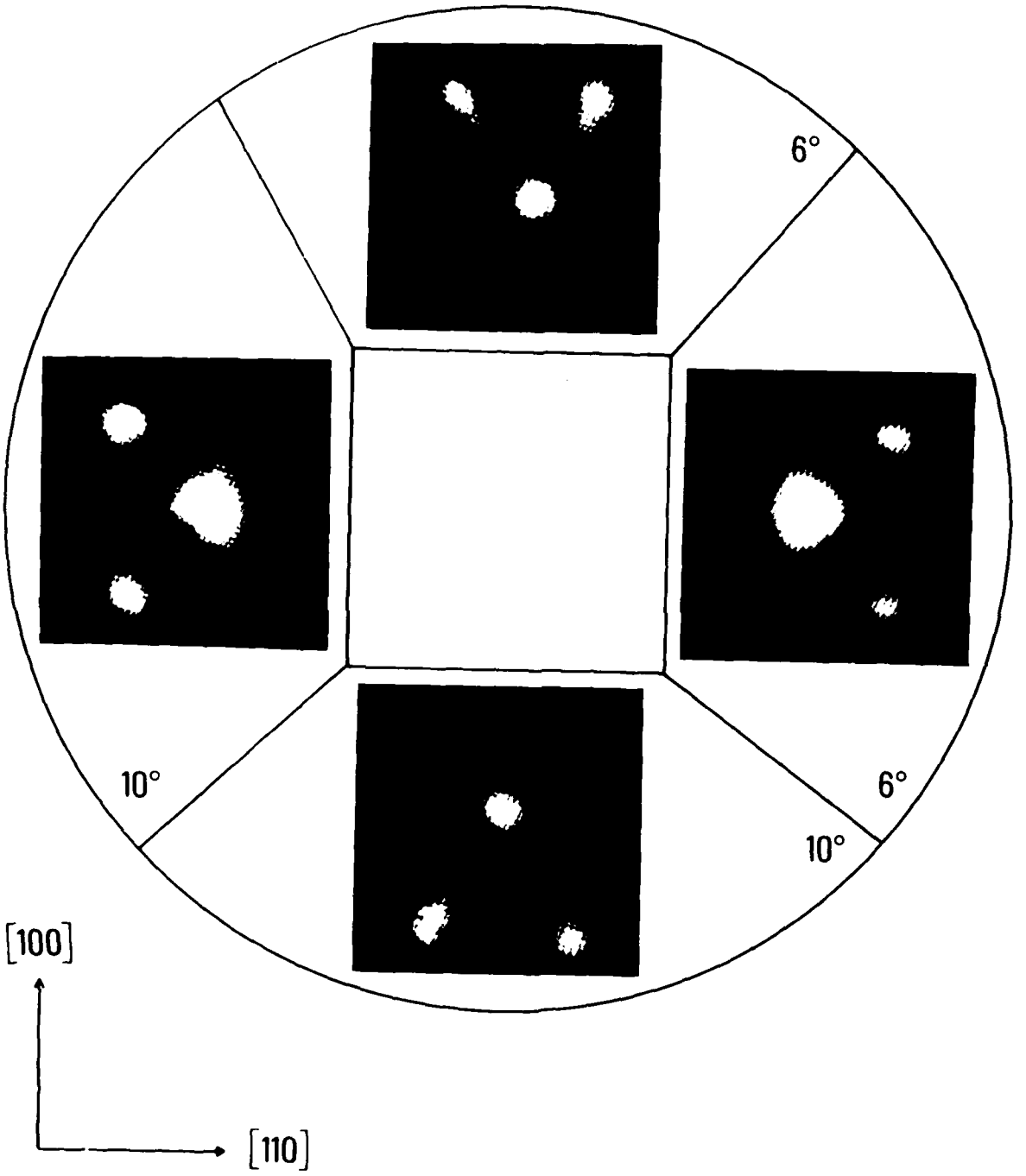

ESDIAD of O^+ From Oxidized, Stepped W(110) Crystal

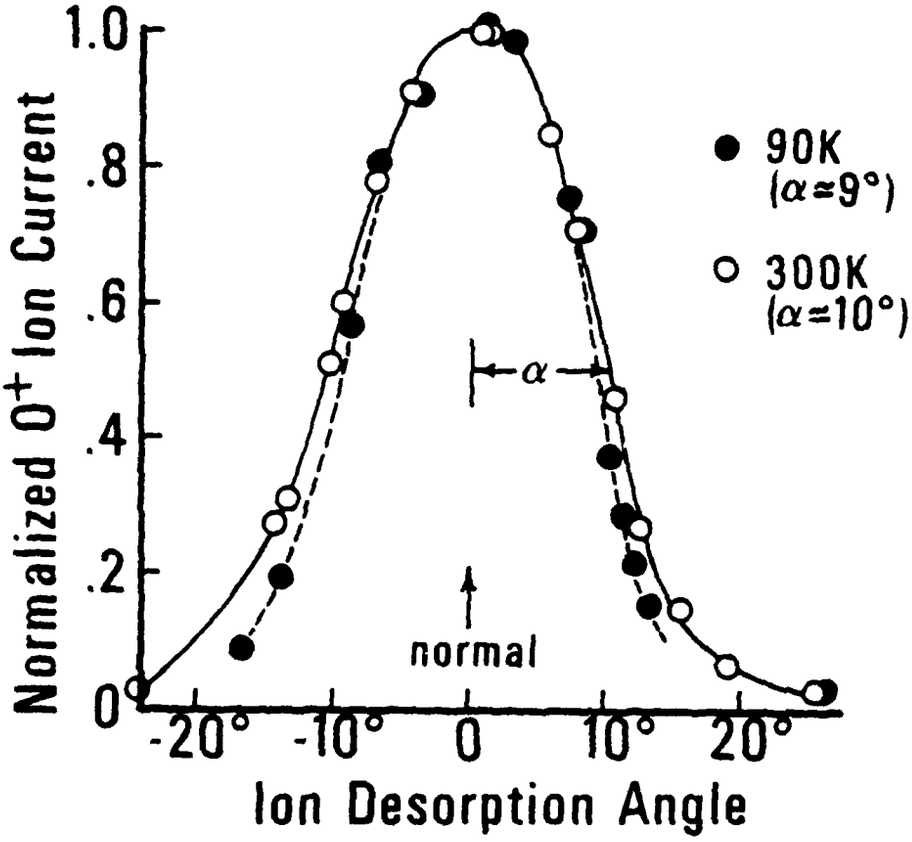

Possible Models for Oxygen Adsorption on stepped Tungsten Crystal